JACS
JOURNAL OF THE AMERICAN CHEMICAL SOCIETY

Article

pubs.acs.org/JACS

Probing a Hidden World of Molecular Self-Assembly: Concentration-Dependent, Three-Dimensional Supramolecular Interconversions

Xiaocun Lu,[†] Xiaopeng Li,[‡,§] Kai Guo,[†] Ting-Zheng Xie,[†] Charles N. Moorefield,[†] Chrys Wesdemiotis,*[,†,‡] and George R. Newkome*[,†,‡]

Departments of [†]Polymer Science and [‡]Chemistry, The University of Akron, 170 University Cr., Akron, Ohio 44325, United States

Supporting Information

ABSTRACT: A terpyridine-based, concentration-dependent, facile self-assembly process is reported, resulting in two three-dimensional metallosupramolecular architectures, a bis-rhombus and a tetrahedron, which are formed using a two-dimensional, planar, tris-terpyridine ligand. The interconversion between these two structures is concentration-dependent: at a concentration higher than 12 mg mL^{-1}, only a bis-rhombus, composed of eight ligands and 12 Cd^{2+} ions, is formed; whereas a self-assembled tetrahedron, composed of four ligands and six Cd^{2+} ions, appears upon sufficient dilution of the tris-terpyridine-metal solution. At concentrations less than 0.5 mg mL^{-1}, only the tetrahedron possessing an S_4 symmetry axis is detected; upon attempted isolation, it quantitatively reverts to the bis-rhombus. This observation opens an unexpected door to unusual chemical pathways under high dilution conditions.

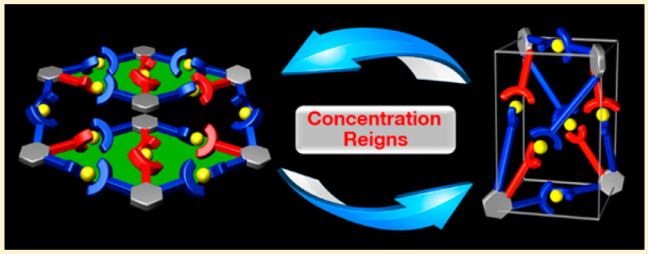

INTRODUCTION

Probing the precise control over the interconversion between different supramolecular assemblies is a great challenge and has recently received notable attention.[1] Critical aspects in the design and construction of supramolecular assemblies include geometric, kinetic, and thermodynamic control.[2] For practical consideration, appropriate external stimuli, such as pH, temperature, and radiation, are efficient to control the supramolecular equilibria.[3] As well, concentration can also play a critical role in some specific self-assembly systems, such as supramolecular aggregation,[4] biological clusters,[5] gelation,[6] and interface assemblies.[7] Such concentration-directed self-assembly is critical to an in-depth understanding of the fundamental aspects in dynamic interactions and may also reveal unobserved chemical pathways under highly dilute conditions.

Three-dimensional, abiological, metallosupramolecular assemblies,[8] such as cages and prisms,[9] have been widely reported and utilized in catalysis,[10] biomedicine,[11] molecular electronics,[12] chemical sensing,[13] and functional materials.[14] In general, there are two major structural considerations in the construction of metallosupramolecular architectures: (a) the metal ions are located at the vertices, and the requisite ligands comprise the edges;[15] and (b) multitopic ligands form the vertices, and metal−ligand connectivity are used for the sides. For the latter, only a few 3D metallosupramolecular architectures,[16] based on ⟨tpy−M^{II}−tpy⟩ (tpy = terpyridine, M = metal) connectivity, have been reported. Concentration is another practical consideration involved in the construction of supramolecular assemblies through coordination connectivity; however, only a few such examples have yet been reported.[17]

Herein, two 3D supramolecular species, a bis-rhombus and a tetrahedron, are reported, in which formation is predicated on a concentration-dependent equilibrium (Figure 1) using a highly

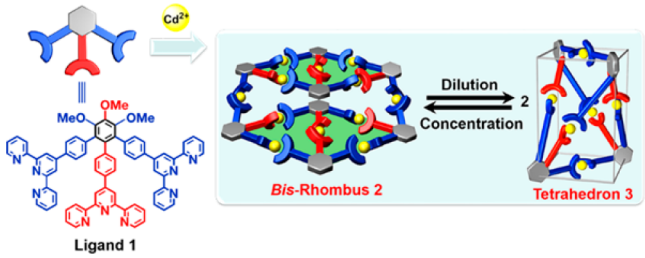

Figure 1. Self-assembly of tris-terpyridine building block **1** gives either a bis-rhombus **2** or a tetrahedral structure **3** depending on concentration.

rigid, tripod-like, deformation of a planar, two-dimensional tris-terpyridine ligand, as vertices. The tetrahedral structure, to the best of our knowledge, is the first example of a coordination-directed, 3D, supramolecular assembly that exists only under dilute conditions.

RESULTS AND DISCUSSION

A terpyridine-based, supramolecular bis-rhombus has recently been formed by combining ligand **1** and Zn^{2+} ions in the stoichiometric ratio of 2:3.[18] In the present case, substitution of Cd^{2+} for Zn^{2+} also formed the architecturally identical bis-

Received: November 5, 2014
Published: December 3, 2014

   dx.doi.org/10.1021/ja511341z | J. Am. Chem. Soc. 2014, 136, 18149−18155

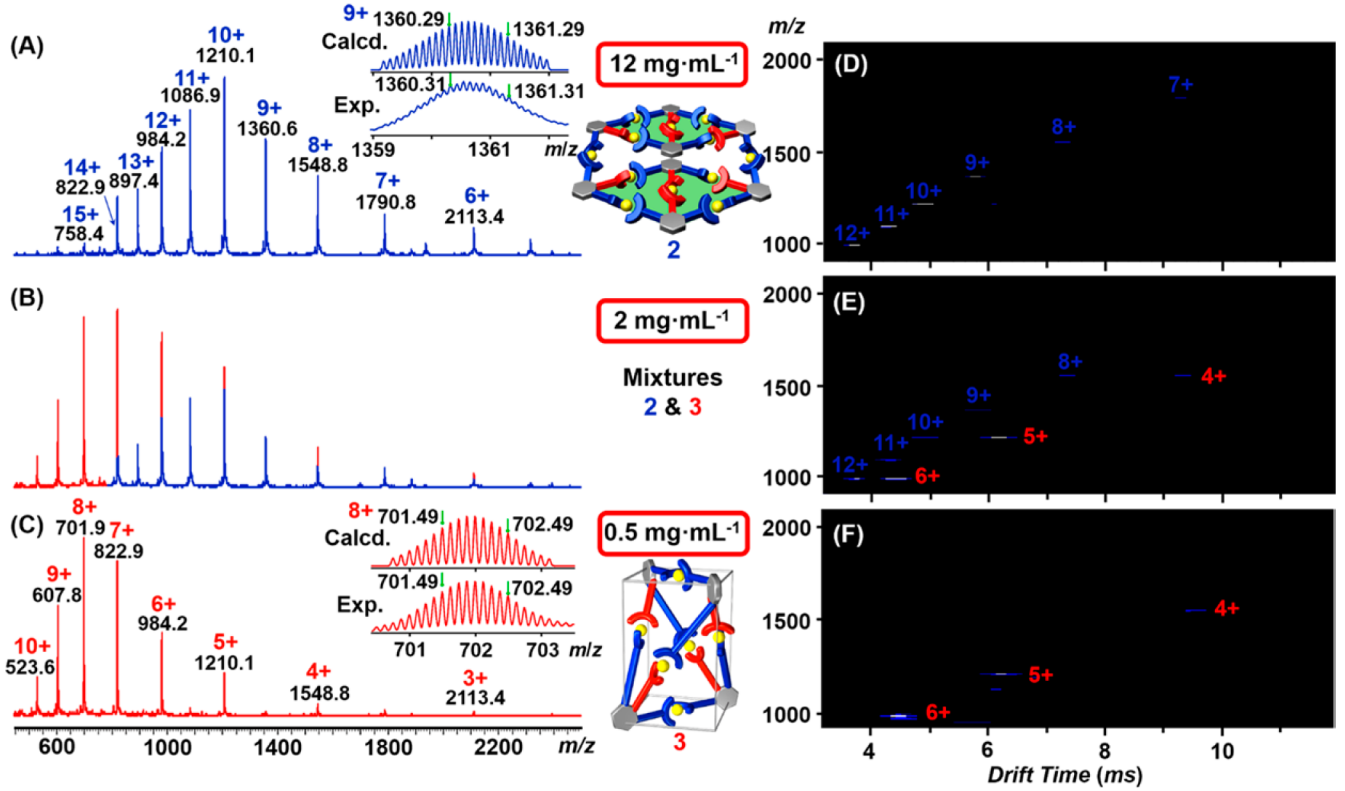

Figure 2. ESI-MS of (A) bis-rhombus **2** (12 mg mL^{-1} in MeCN), (B) mixture of **2** and **3** (2 mg mL^{-1} in MeCN), and (C) tetrahedron **3** (0.5 mg mL^{-1} in MeCN); 2D ESI-TWIM-MS plot (*m/z vs* drift time) for (D) bis-rhombus **2** (12 mg mL^{-1} in MeCN), (E) mixture of **2** and **3** (2 mg mL^{-1} in MeCN), and (F) tetrahedron **3** (0.5 mg mL^{-1} in MeCN). Charge states of intact assemblies are marked.

rhombus structure **2** (Figure 1). Preparation was achieved by mixing ligand **1**[19] with $Cd(NO_3)_2{\cdot}4H_2O$ in a precise 2:3 molar ratio in MeOH and stirring at 65 °C for 3 h, followed by cooling to 25 °C, and then addition of excess NH_4PF_6 to give **2** (>90%); thorough washing with water removed excess inorganic salts. The resultant light-yellow powder was dried *in vacuo* at 50 °C for 12 h, and characterized directly by ESI-MS and NMR experiments (12 mg mL^{-1}; MeCN or CD_3CN, respectively).

The ESI-MS spectrum of complex **2** (Figure 2A) exhibited a series of peaks with charge states from 6+ to 15+ derived by the successive loss of PF_6^- counterions; on the basis of the mass-to-charge (*m/z*) ratios of these ions, the molecular weight for **2** is 13 550.4 Da, confirming that this complex is composed of precisely eight tristerpyridine ligands (*i.e.*, **1**), 12 Cd^{2+} ions, and 24 PF_6^- counterions. Isotope patterns for each charge state agreed well with the corresponding simulated isotope patterns, further supporting the complex's constitution. The ESI-TWIM-MS[20] plot further corroborated the mentioned structural assignment (Figure 2D) by exhibiting a single band with narrow drift time distribution for each charge state, indicating that no other structural conformers, isomers, or other components were present.

The wheel-like complex **2** was also characterized by ^1H NMR spectroscopy (Figure 3A), which showed seven different tpy units with the expected integration ratio, albeit with noticeable yet resolvable peak overlap, which is consistent with the assigned bis-rhomboidal structure (Figure 3A; each tpy unit is represented by a different color and assigned with letters from A to G; full assignment was included in Supporting Information Figures S6 and S19). While the aromatic region of the ^1H NMR

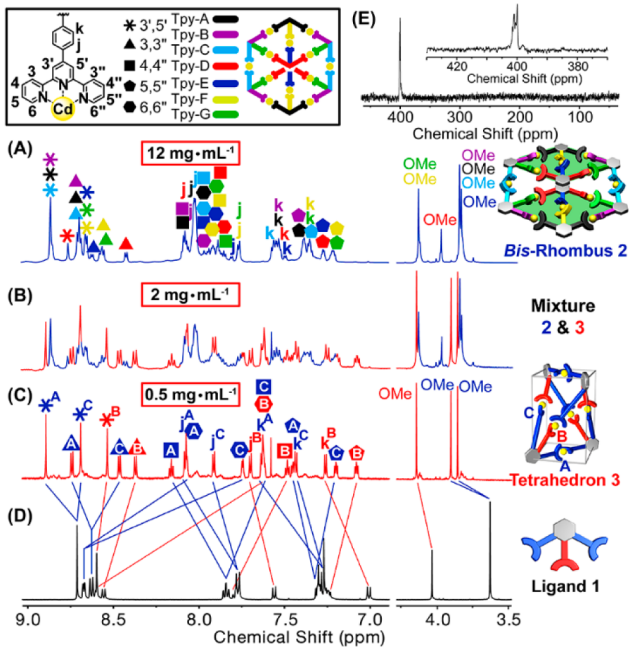

Figure 3. ^1H NMR spectra (CD_3CN, 750 MHz) of (A) bis-rhombus **2** (12 mg mL^{-1}), (B) mixture of **2** and **3** (2 mg·mL^{-1}), (C) tetrahedron **3** (0.5 mg·mL^{-1}); (D) ^1H NMR spectra ($CDCl_3$, 750 MHz) of tris-terpyridine ligand **1**, and (E) ^{113}Cd NMR spectra (CD_3CN, 110 MHz) for bis-rhombus **2** (20 mg mL^{-1}). For the bis-rhombus **2** and the tetrahedron **3**, different tpy units are denoted by the corresponding letter assignments A–G or A–C, respectively (Supporting Information Figure S6).

dx.doi.org/10.1021/ja511341z | J. Am. Chem. Soc. 2014, 136, 18149–18155

spectrum was complicated due to substantial overlap of peaks arising from the different tpy moieties, assignment of the peaks was readily achieved on the basis of the analysis of high resolution (750 MHz) 2D COSY and 2D NOESY NMR spectra (see Supporting Information). Pertinent aspects of these spectra include the observation that all of the 6,6″ protons from the tpy units were significantly shifted upfield due to electron shielding effects, as is typical for the inherent pseudo-octahedral connectivity of the ⟨tpy−Cd^{II}−tpy⟩ components. Further, in the nonaromatic region, the critical OMe markers of **2** exhibited two singlets at 3.99 and 3.86 ppm that were assigned to $H^{OMe\text{-}D}$ and $H^{OMe\text{-}E}$, respectively, with a 2:1 integration ratio, along with two multiplets attributed to the overlapping peaks of the remaining OMe groups. The ^{113}Cd NMR of **2** (Figure 3E) exhibited four peaks at 401.61, 401.02, 400.60, and 400.15 ppm with a 1:2:1:2 integration ratio that is also consistent with the assigned structure in which 12 Cd^{2+} ions reside in four different structural environments.

Following the unequivocal MS and NMR structural confirmation of the Cd^{2+}-based, bis-rhombus **2**, a concentration-dependent phenomenon afforded insight into its possible formation. Upon dilution, **2** was transformed into a smaller novel structure, as recorded in both ESI-MS and NMR studies. Thus, when the concentration was reduced from 12 to 2 mg mL^{-1}, the ESI-MS spectrum revealed that the relative intensity of odd charge states (7+, 9+, 11+, and 13+) was reduced, while the even charge states (6+, 8+, 10+, 12+, and 14+) increased in relative intensity, as a new pattern of charge distribution appeared (Figure 2B). A further reduction in concentration to 0.5 mg mL^{-1} led to a complete disappearance of the original charge states from **2** and the appearance of a completely new series of peaks with charge states from 3+ to 10+ (Figure 2C). The molecular weight deduced from these peaks for the newly formed structure **3** was 6775.2 Da, which is *exactly half* of the molecular weight of **2**, indicating that **3** is composed of precisely four ligands (**1**), six Cd^{2+} ions, and 12 PF_6^- anions. Each charge state is due to the loss of a different number of PF_6^-counterions. The isotope patterns further confirmed the molecular weight difference (see Supporting Information). For the same m/z, the charge states of **3** were always half of those recorded for **2**, supporting the observation that **3** possessed a molecular weight of 6775.2 Da. ESI-TWIM-MS (Figure 2E) clearly confirmed that there were two series of charge states arising from the coexistence of two different structures at 2 mg mL^{-1} and similar intermediate concentrations. The ESI-TWIM-MS plot for **3** (Figure 2F) contained single bands with narrow drift time distributions for all charge states observed, confirming that **3** was composed of a single architectural isomer.

The ^1H NMR also showed the structural changes upon dilution of **2** (Figure 3). When the concentration was reduced from 12 to 2 mg mL^{-1}, a new distinct series of peaks (Figure 3B, red lines) appeared. Upon further dilution, the peaks from **2** (Figure 3A, blue lines) completely disappeared, leaving only the pristine spectrum for the newly formed structure **3** (Figure 3C). The new pattern in the aromatic region showed three different tpy units with equal integration. All of the 6,6″ protons from tpy units were shifted upfield supporting the ⟨tpy−Cd^{II}−tpy⟩ connectivity with no evidence of any uncomplexed tpy moieties. The three singlets at 4.16, 3.91, and 3.87 ppm with equivalent integration were assigned to one set of three different OCH_3 markers. As in the case of complex **2**, all assignments were based on detailed 2D COSY and NOESY analyses (see Supporting Information).

These NMR data provide insight into the connectivity of the newly formed tetrahedral structure **3**; all of the terpyridinyl 6,6″ proton pairs are shifted upfield indicative of 12 coordinated tpy units (four ligands, each with three tpy) via ⟨tpy−Cd^{II}−tpy⟩ linkages. As well, sharp peaks and a simple NMR pattern indicated a high degree-of-molecular-symmetry, suggesting that the pattern of connectivity is unique and not random. Considering that there are three tpy units (tpy^A, tpy^B, tpy^C, Figure 4A) in **1**, tpy^A = tpy^C due to the C_2 symmetry; this was

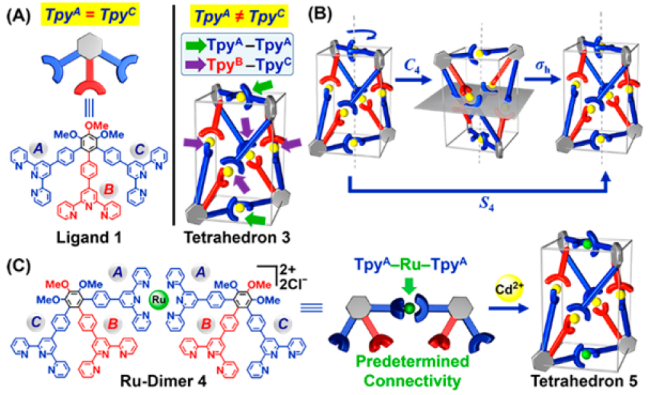

Figure 4. (A) Connectivity pattern of complex **3**; (B) symmetry operations of S_4 symmetry axis in **3**; (C) Ru^{II}-dimer **4** with predetermined connectivity and its corresponding tetrahedron **5**.

confirmed by the distinct 2:1 integration ratio (^1H NMR; Figure 3D) of the two sets of protons from tpy units. However, **3** showed three distinct sets of tpy protons with an 1:1:1 integration ratio; thus, tpy^A and tpy^C are connected, through Cd^{2+}, in different ways. In complex **3**, the tpy^C from one ligand must always be connected with tpy^B from another ligand, while tpy^A from different ligands are always connected with each other (Figure 4A). Alternatively, tpy^B must always be connected with tpy^C, while tpy^A is only connected to another tpy^A. This type of connectivity clearly explains the NMR of the tetrahedron **3** with three different types of tpy units and equivalent integration. The interpretation of the OCH_3 markers also permits insight into the inherent molecular symmetry or asymmetry of the products. Therefore, this newly formed structure **3** is a quasitetrahedron containing only the S_4 symmetry element only[21] (Figure 4B) and possesses three sets of tpy units giving rise to three different singlets from three different juxtaposed methoxy groups per each hexasubstituted apical phenyl moiety.

To further confirm the connectivity pattern within **3**, Ru^{II}-dimer **4** (Figure 4C) was synthesized in 6 steps from commercially available trimethoxybenzene (synthetic route was shown in Supporting Information Figure S9 and experimental details were also included in the Supporting Information), which resulted in two tpy^A units from two tris-terpyridine ligands **1** being connected via stable ⟨tpy−Ru^{II}−tpy⟩ connectivity. When **4** self-assembled with Cd^{2+} ions in MeOH under identical conditions, the connectivity pattern of tpy^A is uniquely predetermined. Thus, if the ligand connectivity pattern based on NMR and MS data (shown in Figure 4A) is correct for **3**, use of dimer **4** would give rise to a similar tetrahedron cage **5** with a nearly identical spectral-derived connectivity pattern. Accordingly, the ESI-MS spectrum of cage

dx.doi.org/10.1021/ja511341z | J. Am. Chem. Soc. 2014, 136, 18149−18155

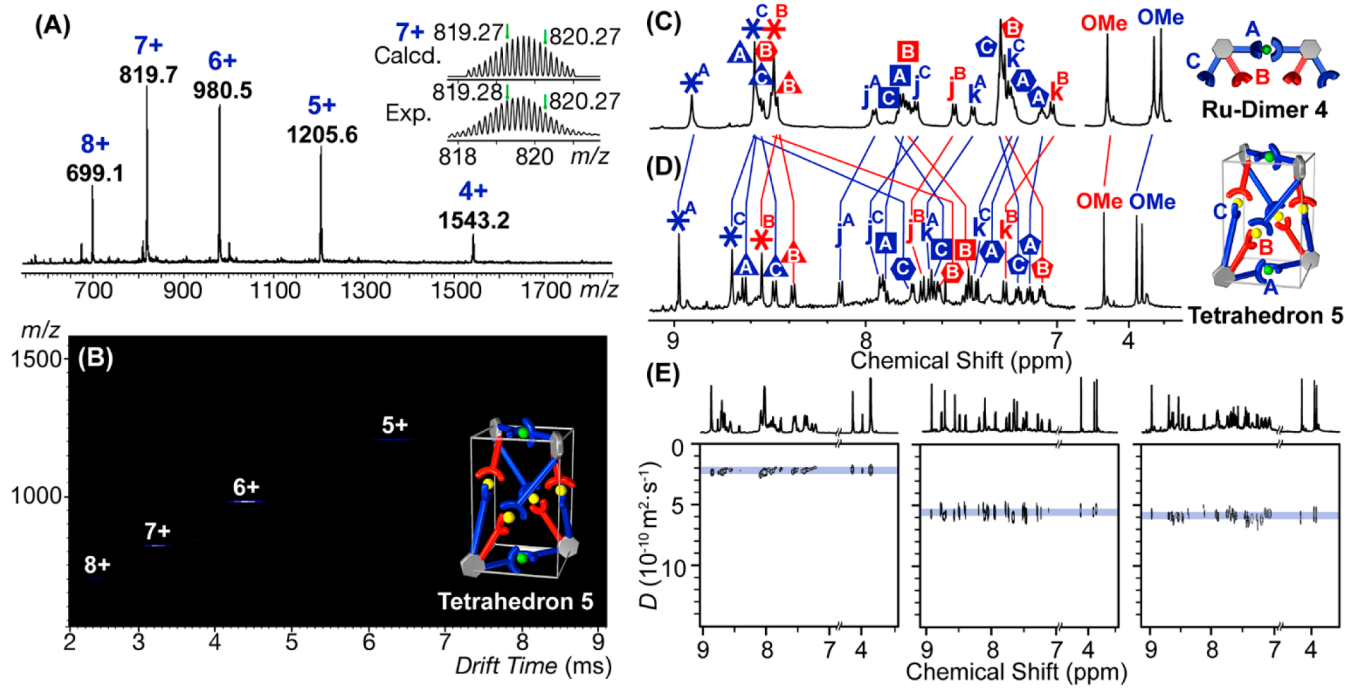

Figure 5. (A) ESI-MS spectrum of **5**. (B) 2D ESI-TWIM-MS plot (*m/z* vs drift time) for **5**. The charge states of intact assemblies are marked. ^{1}H NMR spectra (CD_3CN, 500 MHz) of (C) Ru^{II}-dimer **4** and its (D) corresponding tetrahedron **5**. DOSY NMR spectra (CD_3CN, 500 MHz) of bis-rhombus **2** (E, left), tetrahedron **3** (E, middle), and tetrahedron **5** (E, right).

5 (Figure 5A) exhibited a series of peaks with charge states from 4+ to 8+ derived by the loss of an increasing number of PF_6^- units. From these ions, the molecular weight of **5** was determined to be 6752.7 Da, supporting its composition of precisely two building blocks of dimer **4** (each containing one Ru^{2+}), four Cd^{2+} ions, and 12 PF_6^- anions. Isotope patterns of each charge state agreed well with the corresponding simulated isotope patterns. The ESI-TWIM-MS plot (Figure 5B) further confirmed the structural composition exhibiting charge states with narrow drift time distributions indicating that no other structural conformers or isomers were present. Notably, ^{1}H NMR analysis of tetrahedron **5** (Figure 5D) also revealed three sets of tpy units with equal integration and upfield shifted 6,6″ protons for all tpy units, thereby supporting the presence of ⟨tpy−M^{II}−tpy⟩ (M = Cd or Ru) and no uncomplexed tpy moieties. Assignments were based on detailed analyses of the 2D COSY and NOESY spectra (see Supporting Information).

In diffusion-ordered NMR spectroscopy (DOSY, Figure 5E), all of the signals exhibit a narrow band near diffusion coefficients of 2.6×10^{-10}, 5.5×10^{-10}, and 5.6×10^{-10} m^2 s^{-1} for bis-rhombus **2**, tetrahedron **3**, and tetrahedron **5**, respectively, affirming that the size of the tetrahedron is appreciably smaller compared to bis-rhombus **2**. The sizes of tetrahedra **3** and **5** are very similar, consistent with the common connectivity type in both structures.

Collision cross sections (CCSs) were also derived for several of the ions observed in the TWIM-MS experiments (Table 1). The CCS of an ion is a physical property and represents a measure of the corresponding ion size and architecture. The CCSs for all charge states of tetrahedron **3** (864.3 ± 38.8 Å^2) were found to be significantly lower than the CCSs for the charge states of bis-rhombus **2** (1578.4 ± 22.5 Å^2), which is fully consistent with the respective structures. The CCSs for tetrahedrons **3** and **5** are very similar (864.3 ± 38.8 and 859.5 ± 39.5 Å^2, respectively), indicating that these constructs possess similar structures with the same connectivity. Theoretical CCSs were also calculated on the basis of 300 candidate structures for each complex (from molecular dynamics simulations), using trajectory (TJ) and exact hard sphere scattering (EHSS) methods.[22] The TJ model provides a more realistic CCS prediction, especially for larger ions, as it considers both long-range interactions and momentum transfer between the ions and the gas in the ion mobility region.[22] The time required to perform TJ calculations is, however, long; in such cases, the EHSS method, which ignores long-range

Table 1. Experimental and Theoretical Collision Cross Sections (CCSs) of 2, 3, and 5

		collision cross sections (Å^2)		
charge state	drift time (ms)	expt	expt av	calcd av
Bis-Rhombus **2**				
9+	5.69	1552.0	1578.4 ± 22.5	1711.4 ± 41.9 (EHSS[a])
10+	4.78	1567.9		1667.7 ± 48.0 (TJ[b])
11+	4.15	1592.5		
12+	3.61	1601.2		
Tetrahedron **3**				
5+	6.05	892.6	864.3 ± 38.8	826.6 ± 10.7 (EHSS[a])
6+	4.33	891.7		808.5 ± 14.4 (TJ[b])
7+	3.16	862.8		
8+	2.36	809.9		
Tetrahedron **5**				
5+	6.14	899.7	859.5 ± 39.5	826.6 ± 10.7 (EHSS[a])
6+	4.24	881.0		807.8 ± 15.3 (TJ[b])
7+	3.07	847.3		
8+	2.35	810.0		

[a]EHSS (exact hard sphere scattering) method. [b]TJ (trajectory) method (both available in the MOBCAL program).

dx.doi.org/10.1021/ja511341z | J. Am. Chem. Soc. 2014, 136, 18149−18155

interactions, has been frequently employed. Here, both methods were utilized.

For the larger bis-rhombus **2**, the average CCS of the 300 simulated structures obtained by the TJ method (1667.7 ± 48.0 Å^2) agrees reasonably well with the experimentally deduced average CCS. Conversely, for the smaller tetrahedral complexes **3** and **5**, both the EHSS as well as the TJ method predict CCSs that lie within the range of the measured values. It is noteworthy that the CCS calculated for bis-rhombus **2** is approximately twice as large as the CCSs of either tetrahedral complex (**3** or **5**), in agreement with the presence of twice as many ligands and metal ions in the former.

Finally, gradient tandem MS (gMS^2) experiment was performed on charge state 7+ of the assemblies **2** and **3** to examine the intrinsic stability of these complexes (see Supporting Information). The maximum kinetic energies at which **2** and **3** with 7+ charges survived intact after collisional activation with Ar targets were 57 and 27 eV, respectively. The corresponding center-of-mass collision energies, which represent approximate measures of the intrinsic stabilities of the complexes, are 1.27 and 1.30 eV, respectively. Thus, there is no significant stability difference between these complexes, strongly suggesting that there is no enthalpically driven preference to form a certain complex and that entropic reasons dictate why **2** and **3** coexist within a specific or limited concentration range.

CONCLUSIONS

A 3D supramolecular quasitetrahedron **3** was successfully synthesized in near quantitative yield, and its structure was shown to be an elongated quasitetrahedron with a single S_4 symmetry axis, on the basis of the NMR and MS analysis. Interestingly, the formation of **3** was concentration-dependent, and this complex could only be detected at solution concentrations below 12 mg mL^{-1} and became the only observed assembly below 0.5 mg mL^{-1}. Concentrating a dilute solution, in order to isolate product **3**, shifted the structural equilibrium to the bis-rhombus **2**, suggesting that the S_4 quasitetrahedron exists under these conditions *only at low concentration* (experimental details concerning this experiment along with an initial speciation analysis are reported in Supporting Information). Alternatively, **3** may become an unstable intermediate that fragments to generate a species with one or more broken ⟨tpy−Cd−tpy⟩ connections, which then dimerize to regenerate the more stable, isolated bis-rhombus **2** at higher concentrations. It would thus appear that in the world of 3D supramolecular assembly different unobserved chemical pathways are possible under high dilution conditions. It is worth noting that concentration-dependent aggregation is observed for proteins. Our study documented that such a phenomenon is also possible with abiotic macromolecules.

ASSOCIATED CONTENT

Supporting Information

Complete experimental procedures and characterization of Cd^{2+}-based complexes **2**, **3**, and **5**, including ^{1}H NMR, ^{13}C NMR, COSY, NOESY, ESI-MS, and TWIM-MS. Detailed synthetic route and procedures of Ru^{II}-dimer **4** and the corresponding characterization. Isotope patterns for all complexes and MALDI-ToF result of **4**. This material is available free of charge via the Internet at http://pubs.acs.org.

AUTHOR INFORMATION

Corresponding Authors

wesdemiotis@uakron.edu
newkome@uakron.edu

Present Address

[§]Department of Chemistry and Biochemistry, Texas State University, San Marcos, Texas 78666, United States.

Notes

The authors declare no competing financial interest.

ACKNOWLEDGMENTS

The authors gratefully acknowledge support from the National Science Foundation (CHE-1151991, G.R.N; CHE-1308307, C.W.) and the Ohio Board of Regents.

REFERENCES

(1) (a) Hu, X.-Y.; Xiao, T.; Lin, C.; Huang, F.; Wang, L. *Acc. Chem. Res.* **2014**, *47*, 2041−2051. (b) Klajn, R.; Stoddart, J. F.; Grzybowski, B. A. *Chem. Soc. Rev.* **2010**, *39*, 2203−2237. (c) Lehn, J.-M. *Chem. Soc. Rev.* **2007**, *36*, 151−160. (d) Lehn, J.-M. *Angew. Chem., Int. Ed.* **2013**, *52*, 2836−2850. (e) Saha, M. L.; Pramanik, S.; Schmittel, M. *Chem. Commun.* **2012**, *48*, 9459−9461. (f) Lux, J.; Rebek, J. *Chem. Commun.* **2013**, *49*, 2127−2129.

(2) (a) Chakrabarty, R.; Mukherjee, P. S.; Stang, P. J. *Chem. Rev.* **2011**, *111*, 6810−6918. (b) Cook, T. R.; Zheng, Y.-R.; Stang, P. J. *Chem. Rev.* **2013**, *113*, 734−777. (c) Steed, J. W.; Atwood, J. L. *Supramolecular Chemistry*, 2nd ed.; John Wiley & Sons, Ltd: New York, 2009. (d) Davis, A. V.; Yeh, R. M.; Raymond, K. N. *Proc. Natl. Acad. Sci. U.S.A.* **2002**, *99*, 4793−4796. (e) Turro, N. J. *Proc. Natl. Acad. Sci. U.S.A.* **2005**, *102*, 10765−10765. (f) Gibb, C. L. D.; Gibb, B. C. The thermodynamics of molecular recognition. In *Supramolecular Chemistry*; Gale, P., Steed, J., Eds.; John Wiley & Sons, Ltd: Hoboken, NJ, 2012. (g) Yoneya, M.; Tsuzuki, S.; Yamaguchi, T.; Sato, S.; Fujita, M. *ACS Nano* **2014**, *8*, 1290−1296. (h) Belowich, M. E.; Stoddart, J. F. *Chem. Soc. Rev.* **2012**, *41*, 2003−2024. (i) Dichtel, W. R.; Miljanić, O. Š.; Zhang, W.; Spruell, J. M.; Patel, K.; Aprahamian, I.; Heath, J. R.; Stoddart, J. F. *Acc. Chem. Res.* **2008**, *41*, 1750−1761. (j) Sessler, J. L.; Lawrence, C. M.; Jayawickramarajah, J. *Chem. Soc. Rev.* **2007**, *36*, 314−325. (k) Rambo, B. M.; Gong, H.-Y.; Oh, M.; Sessler, J. L. *Acc. Chem. Res.* **2012**, *45*, 1390−1401. (l) Joyce, L. A.; Shabbir, S. H.; Anslyn, E. V. *Chem. Soc. Rev.* **2010**, *39*, 3621−3632.

(3) Yan, X.; Wang, F.; Zheng, B.; Huang, F. *Chem. Soc. Rev.* **2012**, *41*, 6042−6065.

(4) (a) Tomović, Ž.; van Dongen, J.; George, S. J.; Xu, H.; Pisula, W.; Leclère, P.; Smulders, M. M. J.; De Feyter, S.; Meijer, E. W.; Schenning, A. P. H. J. *J. Am. Chem. Soc.* **2007**, *129*, 16190−16196. (b) Barrett, E. S.; Dale, T. J.; Rebek, J. *J. Am. Chem. Soc.* **2008**, *130*, 2344−2350. (c) Jiao, D.; Biedermann, F.; Tian, F.; Scherman, O. A. *J. Am. Chem. Soc.* **2010**, *132*, 15734−15743. (d) Peterca, M.; Percec, V.; Leowanawat, P.; Bertin, A. *J. Am. Chem. Soc.* **2011**, *133*, 20507−20520.

(5) (a) Wiedman, G.; Fuselier, T.; He, J.; Searson, P. C.; Hristova, K.; Wimley, W. C. *J. Am. Chem. Soc.* **2014**, *136*, 4724−4731. (b) Javid, N.; Vogtt, K.; Roy, S.; Hirst, A. R.; Hoell, A.; Hamley, I. W.; Ulijn, R. V.; Sefcik, J. *J. Phys. Chem. Lett.* **2011**, *2*, 1395−1399.

(6) (a) Ajayaghosh, A.; Varghese, R.; Praveen, V. K.; Mahesh, S. *Angew. Chem., Int. Ed.* **2006**, *45*, 3261−3264. (b) Kumar, N. S. S.; Varghese, S.; Narayan, G.; Das, S. *Angew. Chem., Int. Ed.* **2006**, *45*, 6317−6321.

(7) (a) Voronin, M. A.; Gabdrakhmanov, D. R.; Semenov, V. E.; Valeeva, F. G.; Mikhailov, A. S.; Nizameev, I. R.; Kadirov, M. K.; Zakharova, L. Y.; Reznik, V. S.; Konovalov, A. I. *ACS Appl. Mater. Interfaces* **2011**, *3*, 402−409. (b) Ciesielski, A.; Szabelski, P. J.; Rżysko, W.; Cadeddu, A.; Cook, T. R.; Stang, P. J.; Samorì, P. *J. Am. Chem. Soc.* **2013**, *135*, 6942−6950. (c) Lei, S.; Tahara, K.; De Schryver, F. C.; Van der Auweraer, M.; Tobe, Y.; De Feyter, S. *Angew. Chem., Int. Ed.* **2008**, *47*, 2964−2968. (d) Guo, Z.; De Cat, I.; Van Averbeke, B.; Ghijsens,

E.; Lin, J.; Xu, H.; Wang, G.; Hoeben, F. J. M.; Tomović, Ž.; Lazzaroni, R.; Beljonne, D.; Meijer, E. W.; Schenning, A. P. H. J.; De Feyter, S. *J. Am. Chem. Soc.* **2013**, *135*, 9811−9819.

(8) (a) Northrop, B. H.; Zheng, Y.-R.; Chi, K.-W.; Stang, P. J. *Acc. Chem. Res.* **2009**, *42*, 1554−1563. (b) De, S.; Mahata, K.; Schmittel, M. *Chem. Soc. Rev.* **2010**, *39*, 1555−1575. (c) Li, J.-R.; Yakovenko, A. A.; Lu, W.; Timmons, D. J.; Zhuang, W.; Yuan, D.; Zhou, H.-C. *J. Am. Chem. Soc.* **2010**, *132*, 17599−17610. (d) Li, J.-R.; Zhou, H.-C. *Angew. Chem., Int. Ed.* **2009**, *48*, 8465−8468. (e) Han, M.; Engelhard, D. M.; Clever, G. H. *Chem. Soc. Rev.* **2014**, *43*, 1848−1860. (f) Lehn, J.-M. *Science* **2002**, *295*, 2400−2403. (g) Lehn, J.-M. *Proc. Natl. Acad. Sci. U.S.A.* **2002**, *99*, 4763−4768. (h) Dalgarno, S. J.; Power, N. P.; Atwood, J. L. *Coord. Chem. Rev.* **2008**, *252*, 825−841. (i) Fowler, D. A.; Mossine, A. V.; Beavers, C. M.; Teat, S. J.; Dalgarno, S. J.; Atwood, J. L. *J. Am. Chem. Soc.* **2011**, *133*, 11069−11071. (j) Zuccaccia, D.; Pirondini, L.; Pinalli, R.; Dalcanale, E.; Macchioni, A. *J. Am. Chem. Soc.* **2005**, *127*, 7025−7032. (k) Pinalli, R.; Cristini, V.; Sottili, V.; Geremia, S.; Campagnolo, M.; Caneschi, A.; Dalcanale, E. *J. Am. Chem. Soc.* **2004**, *126*, 6516−6517.

(9) (a) Schmittel, M.; He, B. *Chem. Commun.* **2008**, 4723−4725. (b) Jiménez, A.; Bilbeisi, R. A.; Ronson, T. K.; Zarra, S.; Woodhead, C.; Nitschke, J. R. *Angew. Chem., Int. Ed.* **2014**, *53*, 4556−4560. (c) Riddell, I. A.; Smulders, M. M. J.; Clegg, J. K.; Hristova, Y. R.; Breiner, B.; Thoburn, J. D.; Nitschke, J. R. *Nat. Chem.* **2012**, *4*, 751−756. (d) Stephenson, A.; Argent, S. P.; Riis-Johannessen, T.; Tidmarsh, I. S.; Ward, M. D. *J. Am. Chem. Soc.* **2011**, *133*, 858−870. (e) Granzhan, A.; Schouwey, C.; Riis-Johannessen, T.; Scopelliti, R.; Severin, K. *J. Am. Chem. Soc.* **2011**, *133*, 7106−7115. (f) Bilbeisi, R. A.; Clegg, J. K.; Elgrishi, N.; Hatten, X. d.; Devillard, M.; Breiner, B.; Mal, P.; Nitschke, J. R. *J. Am. Chem. Soc.* **2012**, *134*, 5110−5119. (g) Yamanaka, M.; Kawaharada, M.; Nito, Y.; Takaya, H.; Kobayashi, K. *J. Am. Chem. Soc.* **2011**, *133*, 16650−16656. (h) Zheng, Y.-R.; Zhao, Z.; Wang, M.; Ghosh, K.; Pollock, J. B.; Cook, T. R.; Stang, P. J. *J. Am. Chem. Soc.* **2010**, *132*, 16873−16882. (i) Mirtschin, S.; Slabon-Turski, A.; Scopelliti, R.; Velders, A. H.; Severin, K. *J. Am. Chem. Soc.* **2010**, *132*, 14004−14005. (j) Fan, J.; Lal, S. M.; Song, B.; Schoenherr, H.; Schmittel, M. *J. Am. Chem. Soc.* **2012**, *134*, 150−153. (k) Shi, Y.; Sánchez-Molina, I.; Cao, C.; Cook, T. R.; Stang, P. J. *Proc. Natl. Acad. Sci. U.S.A.* **2014**, *111*, 9390−9395. (l) Chepelin, O.; Ujma, J.; Wu, X.; Slawin, A. M. Z.; Pitak, M. B.; Coles, S. J.; Michel, J.; Jones, A. C.; Barran, P. E.; Lusby, P. J. *J. Am. Chem. Soc.* **2012**, *134*, 19334−19337. (m) Chepelin, O.; Ujma, J.; Barran, P. E.; Lusby, P. J. *Angew. Chem., Int. Ed.* **2012**, *51*, 4194−4197. (n) Lusby, P. J.; Muller, P.; Pike, S. J.; Slawin, A. M. Z. *J. Am. Chem. Soc.* **2009**, *131*, 16398−16400. (o) Engelhard, D. M.; Freye, S.; Grohe, K.; John, M.; Clever, G. H. *Angew. Chem., Int. Ed.* **2012**, *51*, 4747−4750. (p) Frank, M.; Hey, J.; Balcioglu, I.; Chen, Y.-S.; Stalke, D.; Suenobu, T.; Fukuzumi, S.; Frauendorf, H.; Clever, G. H. *Angew. Chem., Int. Ed.* **2013**, *52*, 10102−10106. (q) Hiraoka, S.; Yamauchi, Y.; Arakane, R.; Shionoya, M. *J. Am. Chem. Soc.* **2009**, *131*, 11646−11647. (r) Nakamura, T.; Ube, H.; Miyake, R.; Shionoya, M. *J. Am. Chem. Soc.* **2013**, *135*, 18790−18793. (s) Zheng, Y.-R.; Lan, W.-J.; Wang, M.; Cook, T. R.; Stang, P. J. *J. Am. Chem. Soc.* **2011**, *133*, 17045−17055. (t) Wang, M.; Zheng, Y.-R.; Ghosh, K.; Stang, P. J. *J. Am. Chem. Soc.* **2010**, *132*, 6282−6283. (u) Ghosh, K.; Hu, J.; White, H. S.; Stang, P. J. *J. Am. Chem. Soc.* **2009**, *131*, 6695−6697. (v) Tidmarsh, I. S.; Faust, T. B.; Adams, H.; Harding, L. P.; Russo, L.; Clegg, W.; Ward, M. D. *J. Am. Chem. Soc.* **2008**, *130*, 15167−15175.

(10) (a) Ballester, P.; Vidal-Ferran, A.; van Leeuwen, P. W. N. M. Modern strategies in supramolecular catalysis. In *Advances in Catalysis*; Bruce, C. G., Helmut, K., Eds.; Elsevier Inc.: New York, 2011; Vol. *54*, pp 63−126. (b) Zhao, C.; Sun, Q.-F.; Hart-Cooper, W. M.; DiPasquale, A. G.; Toste, F. D.; Bergman, R. G.; Raymond, K. N. *J. Am. Chem. Soc.* **2013**, *135*, 18802−18805. (c) Zhao, C.; Toste, F. D.; Raymond, K. N.; Bergman, R. G. *J. Am. Chem. Soc.* **2014**, *136*, 14409−14412. (d) Inokuma, Y.; Kawano, M.; Fujita, M. *Nat. Chem.* **2011**, *3*, 349−358. (e) Wang, Z. J.; Brown, C. J.; Bergman, R. G.; Raymond, K. N.; Toste, F. D. *J. Am. Chem. Soc.* **2011**, *133*, 7358−7360. (f) Pluth, M. D.; Bergman, R. G.; Raymond, K. N. *Science* **2007**, *316*, 85−88. (g) Bruns, C. J.; Fujita, D.; Hoshino, M.; Sato, S.; Stoddart, J. F.; Fujita, M. *J. Am. Chem. Soc.* **2014**, *136*, 12027−12034.

(11) (a) Cook, T. R.; Vajpayee, V.; Lee, M. H.; Stang, P. J.; Chi, K.-W. *Acc. Chem. Res.* **2013**, *46*, 2464−2474. (b) Wang, Z. J.; Clary, K. N.; Bergman, R. G.; Raymond, K. N.; Toste, F. D. *Nat. Chem.* **2013**, *5*, 100−103. (c) Zhao, D.; Tan, S.; Yuan, D.; Lu, W.; Rezenom, Y. H.; Jiang, H.; Wang, L.-Q.; Zhou, H.-C. *Adv. Mater.* **2011**, *23*, 90−93.

(12) (a) Moulin, E.; Cid, J.-J.; Giuseppone, N. *Adv. Mater.* **2013**, *25*, 477−487. (b) Winter, A.; Newkome, G. R.; Schubert, U. S. *ChemCatChem* **2011**, *3*, 1384−1406. (c) Fukuzumi, S.; Ohkubo, K.; D'Souza, F.; Sessler, J. L. *Chem. Commun.* **2012**, *48*, 9801−9815.

(13) Kumar, A.; Sun, S.-S.; Lees, A. J. *Coord. Chem. Rev.* **2008**, *252*, 922−939.

(14) (a) Liu, K.; Kang, Y.; Wang, Z.; Zhang, X. *Adv. Mater.* **2013**, *25*, 5530−5548. (b) Schneider, H.-J. *Applications of Supramolecular Chemistry*; CRC Press: Boca Raton, FL, 2012. (c) Ousaka, N.; Grunder, S.; Castilla, A. M.; Whalley, A. C.; Stoddart, J. F.; Nitschke, J. R. *J. Am. Chem. Soc.* **2012**, *134*, 15528−15537. (d) Castilla, A. M.; Ousaka, N.; Bilbeisi, R. A.; Valeri, E.; Ronson, T. K.; Nitschke, J. R. *J. Am. Chem. Soc.* **2013**, *135*, 17999−18006. (e) Castilla, A. M.; Ramsay, W. J.; Nitschke, J. R. *Acc. Chem. Res.* **2014**, *47*, 2063−2073. (f) Mal, P.; Breiner, B.; Rissanen, K.; Nitschke, J. R. *Science* **2009**, *324*, 1697−1699. (g) Li, J.-R.; Yu, J.; Lu, W.; Sun, L.-B.; Sculley, J.; Balbuena, P. B.; Zhou, H.-C. *Nat. Commun.* **2013**, *4*, 1538. (h) Winter, A.; Hager, M. D.; Newkome, G. R.; Schubert, U. S. *Adv. Mater.* **2011**, *23*, 5728−5748. (i) Winter, A.; Hoeppener, S.; Newkome, G. R.; Schubert, U. S. *Adv. Mater.* **2011**, *23*, 3484−3498. (j) Wild, A.; Winter, A.; Schluetter, F.; Schubert, U. S. *Chem. Soc. Rev.* **2011**, *40*, 1459−1511. (k) Schubert, U. S.; Winter, A.; Newkome, G. R. *Terpyridine-Based Materials*. Wiley-VCH: New York, 2011. (l) Rebek, J. *Angew. Chem., Int. Ed.* **2005**, *44*, 2068−2078. (m) Hof, F.; Craig, S. L.; Nuckolls, C.; Rebek, J. J. *Angew. Chem., Int. Ed.* **2002**, *41*, 1488−1508.

(15) (a) Yoshizawa, M.; Klosterman, J. K.; Fujita, M. *Angew. Chem., Int. Ed.* **2009**, *48*, 3418−3438. (b) Pluth, M. D.; Bergman, R. G.; Raymond, K. N. *Acc. Chem. Res.* **2009**, *42*, 1650−1659. (c) Sato, S.; Iida, J.; Suzuki, K.; Kawano, M.; Ozeki, T.; Fujita, M. *Science* **2006**, *313*, 1273−1276. (d) Sun, Q.-F.; Iwasa, J.; Ogawa, D.; Ishido, Y.; Sato, S.; Ozeki, T.; Sei, Y.; Yamaguchi, K.; Fujita, M. *Science* **2010**, *328*, 1144−1147. (e) Sun, Q.-F.; Sato, S.; Fujita, M. *Nat. Chem.* **2012**, *4*, 330−333. (f) Sun, Q.-F.; Murase, T.; Sato, S.; Fujita, M. *Angew. Chem., Int. Ed.* **2011**, *50*, 10318−10321. (g) Saha, M. L.; De, S.; Pramanik, S.; Schmittel, M. *Chem. Soc. Rev.* **2013**, *42*, 6860−6909.

(16) (a) Wang, C.; Hao, X.-Q.; Wang, M.; Guo, C.; Xu, B.; Tan, E. N.; Zhang, Y.-Y.; Yu, Y.; Li, Z.-Y.; Yang, H.-B.; Song, M.-P.; Li, X. *Chem. Sci.* **2014**, *5*, 1221−1226. (b) Schröder, T.; Brodbeck, R.; Letzel, M. C.; Mix, A.; Schnatwinkel, B.; Tonigold, M.; Volkmer, D.; Mattay, J. *Tetrahedron Lett.* **2008**, *49*, 5939−5942. (c) Xie, T.-Z.; Liao, S.-Y.; Guo, K.; Lu, X.; Dong, X.; Huang, M.; Moorefield, C. N.; Cheng, S. Z. D.; Liu, X.; Wesdemiotis, C.; Newkome, G. R. *J. Am. Chem. Soc.* **2014**, *136*, 8165−8168. (d) Wang, M.; Wang, C.; Hao, X.-Q.; Li, X.; Vaughn, T. J.; Zhang, Y.-Y.; Yu, Y.; Li, Z.-Y.; Song, M.-P.; Yang, H.-B.; Li, X. *J. Am. Chem. Soc.* **2014**, *136*, 10499−10507.

(17) (a) Yamamoto, T.; Arif, A. M.; Stang, P. J. *J. Am. Chem. Soc.* **2003**, *125*, 12309−12317. (b) Schnebeck, R.-D.; Freisinger, E.; Lippert, B. *Eur. J. Inorg. Chem.* **2000**, *2000*, 1193−1200. (c) Ludlow, J. M., III; Tominaga, M.; Chujo, Y.; Schultz, A.; Lu, X.; Xie, T.; Guo, K.; Moorefield, C. N.; Wesdemiotis, C.; Newkome, G. R. *Dalton Trans.* **2014**, *43*, 9604−9611. (d) Chand, D. K.; Biradha, K.; Kawano, M.; Sakamoto, S.; Yamaguchi, K.; Fujita, M. *Chem.—Asian J.* **2006**, *1*, 82−90. (e) Sakamoto, S.; Fujita, M.; Kim, K.; Yamaguchi, K. *Tetrahedron* **2000**, *56*, 955−964.

(18) Lu, X.; Li, X.; Guo, K.; Wang, J.; Huang, M.; Wang, J.-L.; Xie, T.-Z.; Moorefield, C. N.; Cheng, S. Z. D.; Wesdemiotis, C.; Newkome, G. R. *Chem.—Eur. J.* **2014**, *20*, 13094−13098.

(19) Wang, J.-L.; Li, X.; Lu, X.; Hsieh, I. F.; Cao, Y.; Moorefield, C. N.; Wesdemiotis, C.; Cheng, S. Z. D.; Newkome, G. R. *J. Am. Chem. Soc.* **2011**, *133*, 11450−11453.

(20) (a) Bernstein, S. L.; Dupuis, N. F.; Lazo, N. D.; Wyttenbach, T.; Condron, M. M.; Bitan, G.; Teplow, D. B.; Shea, J.-E.; Ruotolo, B. T.;

Robinson, C. V.; Bowers, M. T. *Nat. Chem.* **2009**, *1*, 326−331. (b) Ruotolo, B. T.; Benesch, J. L. P.; Sandercock, A. M.; Hyung, S.-J.; Robinson, C. V. *Nat. Protoc.* **2008**, *3*, 1139−1152. (c) Scarff, C. A.; Snelling, J. R.; Knust, M. M.; Wilkins, C. L.; Scrivens, J. H. *J. Am. Chem. Soc.* **2012**, *134*, 9193−9198. (d) Thalassinos, K.; Grabenauer, M.; Slade, S. E.; Hilton, G. R.; Bowers, M. T.; Scrivens, J. H. *Anal. Chem.* **2009**, *81*, 248−254. (e) Brocker, E. R.; Anderson, S. E.; Northrop, B. H.; Stang, P. J.; Bowers, M. T. *J. Am. Chem. Soc.* **2010**, *132*, 13486−13494. (f) Anderson, S. E.; Bleiholder, C.; Brocker, E. R.; Stang, P. J.; Bowers, M. T. *Int. J. Mass Spectrom.* **2012**, *330*−*332*, 78−84. (g) Trimpin, S.; Plasencia, M.; Isailovic, D.; Clemmer, D. E. *Anal. Chem.* **2007**, *79*, 7965−7974.

(21) (a) Saalfrank, R. W.; Maid, H.; Scheurer, A.; Puchta, R.; Bauer, W. *Eur. J. Inorg. Chem.* **2010**, *2010*, 2903−2906. (b) Meng, W.; Clegg, J. K.; Thoburn, J. D.; Nitschke, J. R. *J. Am. Chem. Soc.* **2011**, *133*, 13652−13660. (c) Aroulanda, C.; Zimmermann, H.; Luz, Z.; Lesot, P. *J. Chem. Phys.* **2011**, *134*, 134502−134508.

(22) (a) Shvartsburg, A. A.; Jarrold, M. F. *Chem. Phys. Lett.* **1996**, *261*, 86−91. (b) Jarrold, M. F. *Annu. Rev. Phys. Chem.* **2000**, *51*, 179−207. (c) Shvartsburg, A. A.; Liu, B.; Siu, K. W. M.; Ho, K.-M. *J. Phys. Chem. A* **2000**, *104*, 6152−6157.